

Kinematic control design for wheeled mobile robots with longitudinal and lateral slip

Thiago B. Burghi^a, Juliano G. Iossaqui^b and Juan F. Camino^c

^aDepartment of Engineering, University of Cambridge, Cambridge, UK; ^bTechnological Federal University of Paraná — UTFPR, Londrina, PR, Brazil; ^cSchool of Mechanical Engineering, University of Campinas — UNICAMP, Campinas, SP, Brazil.

ARTICLE HISTORY

Compiled May 17, 2021

ABSTRACT

The motion control of wheeled mobile robots at high speeds under adverse ground conditions is a difficult task, since the robots' wheels may be subject to different kinds of slip. This work introduces an adaptive kinematic controller that is capable of solving the trajectory tracking problem of a nonholonomic mobile robot under longitudinal and lateral slip. While the controller can effectively compensate for the longitudinal slip, the lateral slip is a more involved problem to deal with, since nonholonomic robots cannot directly produce movement in the lateral direction. To show that the proposed controller is still able to make the mobile robot follow a reference trajectory under lateral and longitudinal time-varying slip, the solutions of the robot's position and orientation error dynamics are shown to be uniformly ultimately bounded. Numerical simulations are presented to illustrate the robot's performance using the proposed adaptive control law.

KEYWORDS

Mobile robots; wheel slip; kinematics; trajectory tracking problem ; nonlinear control

1. Introduction

In recent years, the development of control design techniques for mobile robots has received considerable attention. Research in this area is justified by the increasing relevance of mobile robotics in socioeconomic activities such as forestry, mining, agriculture, search and rescue, medicine, housework, industry and space exploration (Klancar, Zdesar, Blazic, & Skrjanc, 2017; Nourbakhsh & Siegwart, 2004). The efficient deployment of mobile robots in these activities requires a solution for the robot motion control problem, which in itself presents interesting theoretical challenges (Ibrahim, Abouelsoud, Elbab, & Ogata, 2019; Morin & Samson, 2006; Urakubo, 2015; Wu, Xu, & Yin, 2009). Mobile robot controllers must deal not only with fundamental nonholonomic constraints in the robot model, but also with practical issues such as actuator saturation, sensor measurement noise, and the wheel slip phenomenon.

^aEmail: tbb29@cam.ac.uk (corresponding author)

^bEmail: julianoioassaqui@utfpr.edu.br

^cEmail: camino@fem.unicamp.br

In this context, reference tracking for nonholonomic differential-drive mobile robots subject to wheel slip is an important control problem. In the ideal scenario in which the slip does not occur, this is a well-known problem (Morin & Samson, 2006; Wu et al., 2009; Zhai & Song, 2019). In particular, controller designs for reference tracking based on Lyapunov theory have been successful in tackling the motion problem in the absence of wheel slip (Fukao, Nakagawa, & Adachi, 2000; Jarzebowska, 2008; Panahandeh, Alipour, Tarvirdizadeh, & Hadi, 2019). However, the performance of such controllers significantly deteriorates whenever wheel slippage occurs, leading in many cases to system instability. One solution to this issue is to explicitly incorporate the slip effects into the controller design.

Motion control design methods (Fierro & Lewis, 1997; Fukao et al., 2000) for wheeled mobile robots can be based on either kinetic or kinematic models (Sidek & Sarkar, 2008; Wang & Low, 2008). Wheel slip, which can be longitudinal and lateral, is treated differently in each of these modeling paradigms. In kinetic models, which relate robot pose accelerations to wheel torques, the modeling of the slip phenomenon is in general complex, as it must deal with factors such as wheel temperature, thread pattern, and camber angle. One approach to overcome these issues is to employ empirical or semi-empirical methods to model traction forces. A simpler approach that avoids the complexities of robot kinetics is to work directly with kinematic models, which relate robot pose speeds to wheel angular velocities. In this case, the slip is taken into account by modeling it as a perturbation in the wheel velocities Wang and Low (2008).

When approaching the kinematic reference tracking control problem, one is faced with the question of how to precisely measure the wheel slip so that it can be incorporated into the control law. A popular design strategy consists in uncoupling the problem of reference tracking from that of measuring or estimating the slip (Chen, 2017; Cui, Huang, Liu, Liu, & Sun, 2014; Gao et al., 2014; Michalek, Dutkiewicz, Kielczewski, & Pazderski, 2009; Moosavian & Kalantari, 2008; Ward & Iagnemma, 2008; Zhou, Peng, & Han, 2007). In this strategy, a reference tracking controller that depends explicitly on the slip perturbation is first designed. Then, an estimator or observer is independently designed to provide an estimate of the slip. Since the tracking and estimation problems are posed separately, a closed-loop stability analysis is not in general pursued; instead, performance and stability are assessed experimentally. This was done by Michalek et al. (2009); Ward and Iagnemma (2008); Zhou et al. (2007) using variants of the Kalman filter, and by Cui et al. (2014) using a sliding mode observer. In Chen (2017), a disturbance-observer-based control law is proposed, but it is built on an auxiliary variable that depends on the slip, which cannot be directly measured.

In contrast with this uncoupled design strategy, the papers Iossaqui and Camino (2013); Iossaqui, Camino, and Zampieri (2011); Li, Wang, Chen, Zhu, and Chen (2016) introduce adaptive Lyapunov-based kinematic control laws which are proven to asymptotically stabilize the closed-loop robot pose error dynamics for the particular case of constant longitudinal slip and no lateral slip. While these works provide a stability analysis of the problem, they neglect the possibility that slip perturbations are time-varying. For the particular case of time-varying lateral slip, but neglecting longitudinal wheel slip, this issue has recently been given attention by Ryu and Agrawal (2010), who designed a differential flatness-based controller based on the kinetic model, Thomas, Bandyopadhyay, and Vachhani (2019), who designed a kinematic sliding mode controller, and Shafiei and Monfared (2019), who designed a kinematic H_∞ controller. In these works, the controllers are proven to drive the

tracking error to a neighborhood of the origin.

This work now significantly extends the previous conference paper (Iossaqui & Camino, 2013) by considering both longitudinal and lateral slip, by allowing the slip to be time-varying, and by proving ultimate boundedness of slip estimates for a large class of time-varying reference trajectories. To our knowledge, this is the first time the closed-loop stability properties of a smooth kinematic controller for differential-drive robots is analyzed in all this generality. Our main result proves that, as long as the reference trajectory and longitudinal slip are slowly varying, and the lateral slip is small, the proposed adaptive kinematic control law, based only on the robot pose, ensures that the tracking error and the unknown longitudinal slip estimation error are ultimately bounded by a small bound. Important advantages of the proposed control law are its smoothness and simplicity; the former avoids issues such as chattering while the latter ensures it is easily implemented in practice. Our approach relies on the analysis of the stability properties of the closed-loop system with respect to nonvanishing perturbations caused by time variations in the longitudinal and lateral slip, and can be readily extended to other controller designs found in the literature.

This paper is organized as follows. Section 2 presents the kinematic differential equations that describe the motion of a wheeled mobile robot with longitudinal and lateral wheel slip. Section 3 introduces the adaptive tracking controller that is able to compensate for the slip with a proof of closed-loop stability. Section 4 presents numerical results using the proposed adaptive controllers.

2. Kinematic model of a wheeled mobile robot

This section presents the kinematic model of the wheeled mobile robot, shown in Figure 1, with longitudinal and lateral slip (Gonzales, Fiacchini, Alamo, Guzmán, & Rodriguez, 2009; Iossaqui et al., 2011; Zhou et al., 2007). It is assumed that the robot can be represented by a rigid body with two independently actuated wheels. The pose of the robot is described by its position (x_p, y_p) and its orientation θ_p in an inertial coordinate frame $F_0(x_0, y_0)$. The robot position is given by the coordinate of its geometric center O , which is also the origin of the local coordinate frame $F_1(x_1, y_1)$. The robot orientation is the angle between the x_0 -axis and the x_1 -axis. The spacing between the centerlines of the two wheels is b . The motion of the robot is described by the rotational velocity $\omega = \dot{\theta}_p$ and the translational velocity v . The translational velocity can be decomposed into the forward velocity v_x in the x_1 -axis and the lateral velocity v_y in the y_1 -axis. The angle between v and v_x is α , which is zero in the absence of lateral slip.

In the absence of any slip, the motion of the wheeled mobile robot can be described by the kinematic model

$$\dot{q}_p(t) = S(q_p(t))\eta(t) \quad (1)$$

where the robot pose $q_p(t)$, the velocity vector $\eta(t)$, and the matrix $S(q_p(t))$, are respectively given by

$$q_p(t) = \begin{pmatrix} x_p(t) \\ y_p(t) \\ \theta_p(t) \end{pmatrix}, \quad S(q_p(t)) = \begin{pmatrix} \cos \theta_p(t) & 0 \\ \sin \theta_p(t) & 0 \\ 0 & 1 \end{pmatrix}, \quad \eta(t) = \begin{pmatrix} v_x(t) \\ \omega(t) \end{pmatrix} \quad (2)$$

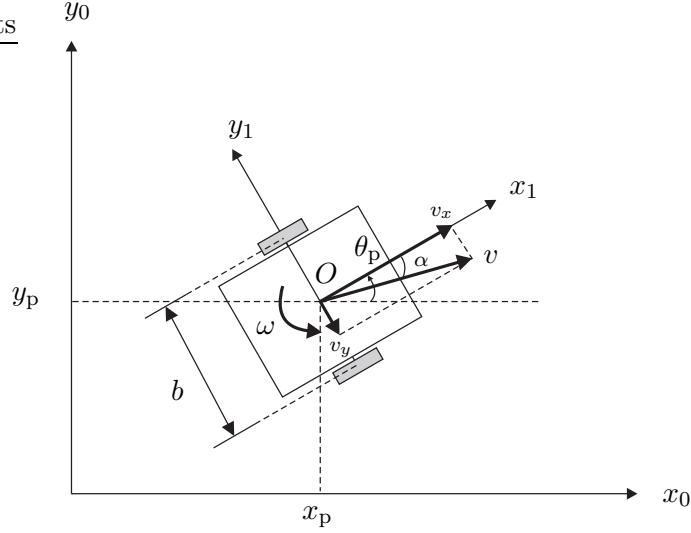


Figure 1. Schematic model of a wheeled mobile robot.

Considering now the lateral slip, the kinematic model becomes

$$\dot{q}_p(t) = S_a(q_p(t))\eta(t) \quad (3)$$

where the matrix $S_a(q_p(t))$ is given by

$$S_a(q_p(t)) = \begin{pmatrix} (\cos \theta_p(t) + \sigma(t) \sin \theta_p(t)) & 0 \\ (\sin \theta_p(t) - \sigma(t) \cos \theta_p(t)) & 0 \\ 0 & 1 \end{pmatrix}$$

and $\sigma(t) := \tan \alpha(t) = v_y(t)/v_x(t)$ denotes the lateral slip.

Although frequently exploited for control design, the robot velocities $v_x(t)$ and $\omega(t)$ cannot be directly used to control a real robot. It is more realistic to define the control input in terms of the angular velocities $\omega_l(t)$ and $\omega_r(t)$ of the left and right wheels, respectively. To relate these two different types of velocities, $v_x(t)$ and $\omega(t)$ are first rewritten as

$$v_x(t) = \frac{v_l(t) + v_r(t)}{2} \quad \text{and} \quad \omega(t) = \frac{v_r(t) - v_l(t)}{b}$$

where $v_l(t)$ and $v_r(t)$ are, respectively, the linear velocities of the left and right wheels.

When longitudinal slip is taken into consideration, the linear velocities $v_l(t)$ and $v_r(t)$ are given by

$$\begin{aligned} v_l(t) &= r\omega_l(t)(1 - i_l(t)), & 0 \leq i_l(t) < 1 \\ v_r(t) &= r\omega_r(t)(1 - i_r(t)), & 0 \leq i_r(t) < 1 \end{aligned}$$

where r is the radius of the wheel and $i_l(t)$ and $i_r(t)$ are, respectively, the longitudinal slip factors of the left and right wheels. When the slip factor is zero, the wheel rolls without slipping (pure rolling). On the other hand, when the slip factor is unity, a

complete slipping of the wheel occurs. Defining the longitudinal slip parameters as

$$a_l(t) = \frac{1}{1 - i_l(t)} \quad \text{and} \quad a_r(t) = \frac{1}{1 - i_r(t)}$$

the following relation between the robot velocities is obtained:

$$\begin{aligned} v_x(t) &= \frac{r}{2} \left(\frac{\omega_l(t)}{a_l(t)} + \frac{\omega_r(t)}{a_r(t)} \right) \\ \omega(t) &= \frac{r}{b} \left(\frac{\omega_r(t)}{a_r(t)} - \frac{\omega_l(t)}{a_l(t)} \right) \end{aligned} \tag{4}$$

Collecting the wheel angular velocities in the vector $\xi(t) = (\omega_l(t), \omega_r(t))^T$, relation (4) can also be expressed as

$$\eta(t) = \Phi(t)\xi(t) \tag{5}$$

with matrix $\Phi(t)$ given by

$$\Phi(t) = \frac{r}{2b} \begin{pmatrix} ba_l^{-1}(t) & ba_r^{-1}(t) \\ -2a_l^{-1}(t) & 2a_r^{-1}(t) \end{pmatrix} \tag{6}$$

Finally, substituting (5) into (1) yields the model

$$\dot{q}_p(t) = S(q_p(t))\Phi(t)\xi(t) \tag{7}$$

which takes into account how longitudinal slip affects the robot kinematics when the lateral slip is neglected. Analogously, substituting (5) into (3) yields the model

$$\dot{q}_p(t) = S_a(q_p(t))\Phi(t)\xi(t) \tag{8}$$

which takes into account how both lateral and longitudinal slip affect the robot kinematics.

Remark 1. Notice that the matrix $\Phi(t)$ in (6) is always nonsingular. Thus, relation (5) can be inverted, giving

$$\xi(t) = \Phi^{-1}(t)\eta(t)$$

or more explicitly

$$\begin{pmatrix} \omega_l(t) \\ \omega_r(t) \end{pmatrix} = \frac{1}{2r} \begin{pmatrix} 2a_l(t) & -ba_l(t) \\ 2a_r(t) & ba_r(t) \end{pmatrix} \begin{pmatrix} v_x(t) \\ \omega(t) \end{pmatrix}$$

Consequently, if the longitudinal slip parameters $a_l(t)$ and $a_r(t)$ are precisely known, the wheel angular velocity vector $\xi(t) = (\omega_l(t), \omega_r(t))^T$ can be precisely obtained from any desired velocity vector $\eta(t) = (v_x(t), \omega(t))^T$. For this reason, $\eta(t)$ will be called the kinematic control input, while $\xi(t)$ will be called the effective control input.

3. Adaptive kinematic control law

This section introduces a trajectory tracking kinematic control law for the robot shown in Figure 1. Section 3.1 poses the trajectory tracking control problem, and recalls some results from the literature concerning the case in which the slip is fully neglected. Section 3.2 introduces our control law and shows that it drives the robot to asymptotically track a broad class of reference trajectories whenever the longitudinal slip is constant and the lateral slip is neglected. The remaining sections are dedicated to showing that this same control law can still solve the trajectory tracking problem when the longitudinal slip and the (non-negligible) lateral slip are slowly time-varying. More precisely, our main result states that the tracking error is uniformly ultimately bounded, in other words, the reference trajectory can be tracked closely (although not asymptotically) by the robot. Section 3.3 presents the main result and its underlying assumptions, and Sections 3.3 and 3.4 provide the details involved in its proof.

3.1. Preliminaries

The goal of the control design problem is to provide an input to the robot such that the robot pose $q_p(t)$ tracks a given reference trajectory $q_{\text{ref}}(t)$. This can be done by enforcing that

$$\lim_{t \rightarrow \infty} (q_{\text{ref}}(t) - q_p(t)) = 0$$

where the reference trajectory $q_{\text{ref}}(t) = (x_{\text{ref}}(t), y_{\text{ref}}(t), \theta_{\text{ref}}(t))^T$ is generated using the kinematic model

$$\dot{q}_{\text{ref}}(t) = S(q_{\text{ref}}(t))\eta_{\text{ref}}(t) \quad (9)$$

with $\eta_{\text{ref}}(t) = (v_{\text{ref}}(t), \omega_{\text{ref}}(t))^T$ the reference input and $S(\cdot)$ the map given by (2).

To ensure that the robot pose $q_p(t)$ will track the reference trajectory $q_{\text{ref}}(t)$, the pose error $e(t) = (e_1(t), e_2(t), e_3(t))^T$ is defined as follows:

$$\begin{pmatrix} e_1(t) \\ e_2(t) \\ e_3(t) \end{pmatrix} = \begin{pmatrix} \cos \theta_p(t) & \sin \theta_p(t) & 0 \\ -\sin \theta_p(t) & \cos \theta_p(t) & 0 \\ 0 & 0 & 1 \end{pmatrix} \begin{pmatrix} x_{\text{ref}}(t) - x_p(t) \\ y_{\text{ref}}(t) - y_p(t) \\ \theta_{\text{ref}}(t) - \theta_p(t) \end{pmatrix} \quad (10)$$

Clearly, the robot pose $q_p(t)$ converges to the reference trajectory $q_{\text{ref}}(t)$ whenever the pose error $e(t)$ converges to zero. Thus, it is possible to solve the trajectory tracking problem by showing that the origin of the pose error dynamics is an asymptotically stable equilibrium point.

Neglecting the longitudinal and the lateral slip, the error dynamics in terms of the kinematic control input $\eta(t) = (v_x(t), \omega(t))^T$ is directly obtained from (1), (9), and (10), as follows:

$$\begin{pmatrix} \dot{e}_1(t) \\ \dot{e}_2(t) \\ \dot{e}_3(t) \end{pmatrix} = \begin{pmatrix} v_{\text{ref}}(t) \cos e_3(t) \\ v_{\text{ref}}(t) \sin e_3(t) \\ \omega_{\text{ref}}(t) \end{pmatrix} + \begin{pmatrix} -1 & e_2(t) \\ 0 & -e_1(t) \\ 0 & -1 \end{pmatrix} \eta(t) \quad (11)$$

Under the hypothesis that the reference inputs ω_{ref} and v_{ref} are constants, the

authors in Kim and Oh (1998) showed that the kinematic control law $\eta(t) = \eta_c(t) = (v_c(t), \omega_c(t))^T$, with

$$\begin{aligned} v_c(t) &= v_{\text{ref}}(t) \cos e_3(t) - k_3 e_3(t) \omega_c(t) + k_1 e_1(t) \\ \omega_c(t) &= \omega_{\text{ref}}(t) + \frac{v_{\text{ref}}(t)}{2} \left[k_2 (e_2(t) + k_3 e_3(t)) + \frac{1}{k_3} \sin e_3(t) \right], \quad k_i > 0 \end{aligned} \quad (12)$$

asymptotically stabilizes the origin of the ideal slip-free error dynamics (11), thus ensuring that the pose error $e(t)$ converges to zero. This fact can be shown using the following Lyapunov function:

$$V(e(t)) = \frac{1}{2} e_1^2(t) + \frac{1}{2} (e_2(t) + k_3 e_3(t))^2 + \frac{(1 - \cos e_3(t))}{k_2} \quad (13)$$

Notice that it is straightforward to take into account the longitudinal slip, while neglecting the lateral slip, by substituting (5) into (11), that is

$$\dot{e}(t) = \begin{pmatrix} v_{\text{ref}}(t) \cos e_3(t) \\ v_{\text{ref}}(t) \sin e_3(t) \\ \omega_{\text{ref}}(t) \end{pmatrix} + \begin{pmatrix} -1 & e_2(t) \\ 0 & -e_1(t) \\ 0 & -1 \end{pmatrix} \Phi(t) \xi(t) \quad (14)$$

Thus, an obvious consequence of Remark 1, which has not been emphasized in the literature, is that any kinematic control law $\eta_c(t)$ such as (12), which stabilizes the origin of the ideal system (11), can also be used to stabilize the origin of the error dynamics (14), as long as the longitudinal slip is precisely known. For this to be accomplished, it suffices to choose the effective control input $\xi(t) = \Phi^{-1}(t) \eta_c(t)$. However, when the longitudinal slip is unknown, one can no longer make use of the matrix $\Phi(t)$ in the control input $\xi(t)$, and this simple approach cannot be applied.

In the next section, the kinematic control law (12) will be exploited in order to derive an effective control law to stabilize the origin of (14) when the longitudinal slip is constant.

3.2. Constant longitudinal slip without lateral slip

For the particular case in which the reference input $\eta_{\text{ref}}(t) = (v_{\text{ref}}(t), \omega_{\text{ref}}(t))^T$ is a piecewise continuous function of time and the longitudinal slip parameters a_l and a_r are unknown constants, it is possible to provide a controller to compensate for the slip by combining the kinematic control law (12) with an adaptive update rule. The key insight is to choose the effective control input as $\xi(t) = \hat{\Phi}^{-1}(t) \eta_c(t)$, where $\hat{\Phi}(t)$ is a matrix constructed by replacing the parameters a_l and a_r in $\Phi(t)$ by their estimates $\hat{a}_l(t)$ and $\hat{a}_r(t)$, respectively, given by

$$\begin{aligned} \hat{a}_l(t) &= a_l + \tilde{a}_l(t) \\ \hat{a}_r(t) &= a_r + \tilde{a}_r(t) \end{aligned} \quad (15)$$

with $\tilde{a}_l(t)$ and $\tilde{a}_r(t)$ the estimation errors. This results in the effective control input

$$\begin{pmatrix} \omega_l(t) \\ \omega_r(t) \end{pmatrix} = \frac{1}{2r} \begin{pmatrix} 2\hat{a}_l(t) & -b\hat{a}_l(t) \\ 2\hat{a}_r(t) & b\hat{a}_r(t) \end{pmatrix} \begin{pmatrix} v_c(t) \\ \omega_c(t) \end{pmatrix} \quad (16)$$

with $\eta_c(t) = (v_c(t), \omega_c(t))^T$ given by (12), and the corresponding kinematic control law $\eta(t) = \Phi(t)\hat{\Phi}^{-1}(t)\eta_c(t)$.

It will now be shown that the adaptive control law (16) asymptotically stabilizes the origin of (14), for constant longitudinal slip parameters, i.e., with $\Phi(t) = \Phi$ a constant matrix. By substituting (15) and (16) into (14), the pose error dynamics after some manipulations is given by

$$\begin{aligned} \dot{e}_1(t) = & \left(1 + \frac{\tilde{a}_r(t)}{a_r}\right) \left(\frac{e_2(t)}{b} - \frac{1}{2}\right) \left(v_c(t) + \frac{b}{2}\omega_c(t)\right) + v_{\text{ref}}(t) \cos e_3(t) \\ & - \left(1 + \frac{\tilde{a}_l(t)}{a_l}\right) \left(\frac{e_2(t)}{b} + \frac{1}{2}\right) \left(v_c(t) - \frac{b}{2}\omega_c(t)\right) \end{aligned} \quad (17)$$

$$\begin{aligned} \dot{e}_2(t) = & \left(1 + \frac{\tilde{a}_l(t)}{a_l}\right) \left(v_c(t) - \frac{b}{2}\omega_c(t)\right) \frac{e_1(t)}{b} + v_{\text{ref}}(t) \sin e_3(t) \\ & - \left(1 + \frac{\tilde{a}_r(t)}{a_r}\right) \left(v_c(t) + \frac{b}{2}\omega_c(t)\right) \frac{e_1(t)}{b} \end{aligned} \quad (18)$$

$$\dot{e}_3(t) = \omega_{\text{ref}}(t) - \frac{1}{b} \left(1 + \frac{\tilde{a}_r(t)}{a_r}\right) \left(v_c(t) + \frac{b}{2}\omega_c(t)\right) + \frac{1}{b} \left(1 + \frac{\tilde{a}_l(t)}{a_l}\right) \left(v_c(t) - \frac{b}{2}\omega_c(t)\right) \quad (19)$$

To obtain an update rule for the slip estimates, the following Lyapunov function candidate is considered

$$V_a(e_a(t)) = V(e(t)) + \frac{\tilde{a}_l^2(t)}{2\gamma_1 a_l} + \frac{\tilde{a}_r^2(t)}{2\gamma_2 a_r}, \quad \gamma_i > 0 \quad (20)$$

with $V(e(t))$ given by (13) and the augmented error defined as $e_a(t) = (e_1, e_2, e_3, \tilde{a}_l, \tilde{a}_r)^T$. Using (17), (18), and (19) and noticing that $\dot{\tilde{a}}_l(t) = \dot{\hat{a}}_l(t)$ and $\dot{\tilde{a}}_r(t) = \dot{\hat{a}}_r(t)$, since a_l and a_r are constant, the derivative of $V_a(e_a(t))$ can be expressed, after some manipulations, as

$$\begin{aligned} \dot{V}_a(e_a(t)) = & -k_1 e_1^2(t) - \frac{v_{\text{ref}}(t)}{2} k_2 k_3 (e_2(t) + k_3 e_3(t))^2 - \frac{v_{\text{ref}}(t)}{2k_2 k_3} \sin^2 e_3(t) \\ & + \frac{\tilde{a}_l(t)}{a_l} \left\{ \frac{\dot{\hat{a}}_l(t)}{\gamma_1} - \left(v_c(t) - \frac{b}{2}\omega_c(t)\right) \left[\left(\frac{e_2(t)}{b} + \frac{1}{2}\right) e_1(t) \right. \right. \\ & \left. \left. - \left(\frac{e_1(t)}{b} + \frac{k_3}{b}\right) (e_2(t) + k_3 e_3(t)) - \frac{1}{bk_2} \sin e_3(t) \right] \right\} \\ & + \frac{\tilde{a}_r(t)}{a_r} \left\{ \frac{\dot{\hat{a}}_r(t)}{\gamma_2} - \left(v_c(t) + \frac{b}{2}\omega_c(t)\right) \left[-\left(\frac{e_2(t)}{b} - \frac{1}{2}\right) e_1(t) \right. \right. \\ & \left. \left. + \left(\frac{e_1(t)}{b} + \frac{k_3}{b}\right) (e_2(t) + k_3 e_3(t)) + \frac{1}{bk_2} \sin e_3(t) \right] \right\} \end{aligned}$$

with $v_c(t)$ and $\omega_c(t)$ given by (12). Now, choosing the update rule for $\hat{a}_l(t)$ and $\hat{a}_r(t)$

as

$$\begin{aligned}
\dot{\hat{a}}_l(t) &= \gamma_1 \left(v_c(t) - \frac{b}{2} \omega_c(t) \right) \left[\left(\frac{e_2(t)}{b} + \frac{1}{2} \right) e_1(t) \right. \\
&\quad \left. - \left(\frac{e_1(t)}{b} + \frac{k_3}{b} \right) (e_2(t) + k_3 e_3(t)) - \frac{1}{bk_2} \sin e_3(t) \right] \\
\dot{\hat{a}}_r(t) &= \gamma_2 \left(v_c(t) + \frac{b}{2} \omega_c(t) \right) \left[- \left(\frac{e_2(t)}{b} - \frac{1}{2} \right) e_1(t) \right. \\
&\quad \left. + \left(\frac{e_1(t)}{b} + \frac{k_3}{b} \right) (e_2(t) + k_3 e_3(t)) + \frac{1}{bk_2} \sin e_3(t) \right]
\end{aligned} \tag{21}$$

it finally follows that

$$\dot{V}_a(e_a(t)) = -k_1 e_1^2(t) - \frac{v_{\text{ref}}(t)}{2} k_2 k_3 (e_2(t) + k_3 e_3(t))^2 - \frac{v_{\text{ref}}(t)}{2k_2 k_3} \sin^2 e_3(t) \tag{22}$$

With this choice of update rule, the dynamics of the augmented error $e_a(t)$ is thus given by

$$\dot{e}_a = f_a(t, e_a(t)) \tag{23}$$

where the rows of f_a are the expressions on the right-hand sides of (17)-(19) and (21), with $\dot{\hat{a}}_l(t) = \dot{\hat{a}}_l(t)$ and $\dot{\hat{a}}_r(t) = \dot{\hat{a}}_r(t)$, and the control input $v_c(t)$ and $\omega_c(t)$ given by (12). At this point, Theorem 8.4 from (Khalil, 2002, p. 323) can be applied to show that the origin of (23) is uniformly asymptotically stable. To see this fact, observe that the function $V_a(e_a(t))$ is positive definite over the domain $D = \{e_a(t) \in \mathbb{R}^5 \mid -\pi < e_3(t) < \pi\}$. In addition, the function $\dot{V}_a(t, e_a(t))$ is bounded above by $-W(e_a(t))$, with $W(e_a(t))$ the positive semidefinite function

$$W(e_a(t)) = k_1 e_1^2(t) + \frac{k_2 k_3 \mu}{2} (e_2(t) + k_3 e_3(t))^2 + \frac{\mu}{2k_2 k_3} \sin^2 e_3(t), \quad 0 < \mu \leq v_{\text{ref}}(t)$$

By noticing that $f_a(t, 0) = 0$, all conditions of Theorem 8.4 are satisfied, which implies that all solutions of (23) are bounded and satisfy $W(e_a(t)) \rightarrow 0$ as $t \rightarrow \infty$. Consequently, $e(t) \rightarrow 0$ as $t \rightarrow \infty$. This conclusion extends a previous result shown in Iossaqui et al. (2011), that dealt with the particular case in which the reference input $\eta_{\text{ref}} = (v_{\text{ref}}, \omega_{\text{ref}})^T$ is restricted to be constant.

Figure 2 shows the schematic representation of the closed-loop system composed of the reference trajectory, the adaptive kinematic control law, and the robot. The numbering inside the blocks indicates the corresponding equation number. The adaptive control law is composed of the kinematic control law $\eta_c = (v_c, \omega_c)^T$ given by (12) together with the update rule given by (21).

The adaptive kinematic control law described in this section was obtained neglecting the lateral slip and assuming constant longitudinal slip parameters. In the next section, using a different approach, it is shown that this same adaptive kinematic control law can also guarantee that the augmented error signal $e_a(t)$ is ultimately bounded for a slow time-varying reference input $\eta_{\text{ref}}(t)$, a sufficiently small lateral slip $\sigma(t)$, and slow time-varying longitudinal slip parameters $a_l(t)$ and $a_r(t)$.

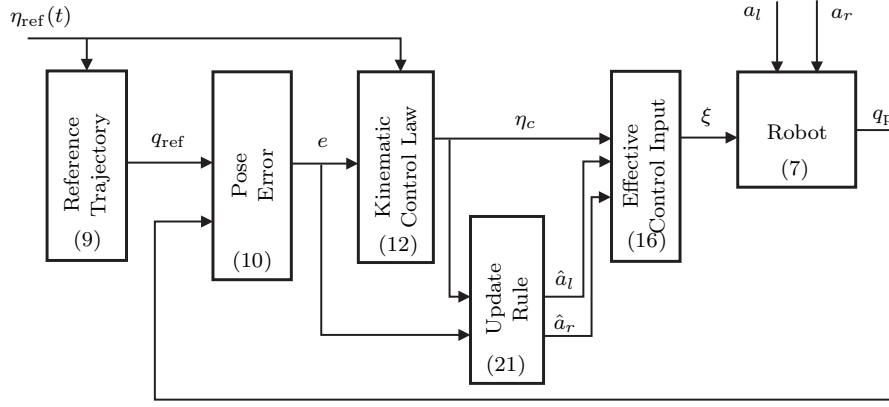


Figure 2. Adaptive kinematic control strategy.

3.3. Time-varying longitudinal and lateral slip

This section extends the stability analysis of the adaptive kinematic control law introduced in Section 3.2 to the case where the longitudinal slip and the (non-negligible) lateral slip are time-varying. More specifically, assuming that the time-varying parameters of the system vary slowly, it will be shown that the proposed control law ensures that the augmented error $e_a(t) = (e_1, e_2, e_3, \tilde{a}_l, \tilde{a}_r)^T$ is ultimately bounded, i.e., it reaches a neighborhood of the origin in finite time, and stays in that neighborhood thereafter.

When the longitudinal slip is time-varying, the estimates are given by

$$\begin{aligned}\hat{a}_l(t) &= a_l(t) + \tilde{a}_l(t) \\ \hat{a}_r(t) &= a_r(t) + \tilde{a}_r(t)\end{aligned}\tag{24}$$

It will be assumed throughout that the slip parameters $a_l(t)$ and $a_r(t)$ are differentiable functions of time. In that case, considering time-varying slip parameters, the dynamics of the augmented error $e_a(t)$, derived using (8), (9), (10), (16), (21), and (24), can be written (after some manipulations) as the following perturbed system:

$$\dot{e}_a(t) = f_a(t, e_a(t)) + g(t, e_a(t)) + g_n(t, e_a(t))\tag{25}$$

with a nominal term $f_a(t, e_a(t))$ given by

$$f_a(t, e_a(t)) = \begin{pmatrix} \Delta_r \Omega_3 \Omega_1 + v_{\text{ref}}(t) \cos e_3(t) - \Delta_l \Omega_4 \Omega_2 \\ \Delta_l \Omega_2 \frac{e_1(t)}{b} + v_{\text{ref}}(t) \sin e_3(t) - \Delta_r \Omega_1 \frac{e_1(t)}{b} \\ \omega_{\text{ref}}(t) - \frac{1}{b} \Delta_r \Omega_1 + \frac{1}{b} \Delta_l \Omega_2 \\ \gamma_1 \Omega_2 \left[\Omega_4 e_1(t) - \left(\frac{e_1(t)}{b} + \frac{k_3}{b} \right) (e_2(t) + k_3 e_3(t)) - \frac{1}{bk_2} \sin e_3(t) \right] \\ \gamma_2 \Omega_1 \left[-\Omega_3 e_1(t) + \left(\frac{e_1(t)}{b} + \frac{k_3}{b} \right) (e_2(t) + k_3 e_3(t)) + \frac{1}{bk_2} \sin e_3(t) \right] \end{pmatrix}$$

where

$$\begin{aligned}\Delta_r &= \left(1 + \frac{\tilde{a}_r(t)}{a_r(t)}\right), & \Omega_1 &= \left(v_c(t) + \frac{b}{2}\omega_c(t)\right), & \Omega_3 &= \left(\frac{e_2(t)}{b} - \frac{1}{2}\right) \\ \Delta_l &= \left(1 + \frac{\tilde{a}_l(t)}{a_l(t)}\right), & \Omega_2 &= \left(v_c(t) - \frac{b}{2}\omega_c(t)\right), & \Omega_4 &= \left(\frac{e_2(t)}{b} + \frac{1}{2}\right)\end{aligned}$$

a vanishing perturbation term $g(t, e_a(t))$ given by

$$g(t, e_a(t)) = \begin{pmatrix} 0 \\ \sigma(t) \left[\frac{1}{2} \frac{\tilde{a}_l(t)}{a_l(t)} \Omega_2 + \frac{1}{2} \frac{\tilde{a}_r(t)}{a_r(t)} \Omega_1 - k_3 e_3(t) \omega_c(t) + k_1 e_1(t) \right] \\ 0 \\ 0 \\ 0 \end{pmatrix}$$

and a nonvanishing perturbation term $g_n(t, e_a(t))$ given by

$$g_n(t, e_a(t)) = \begin{pmatrix} 0 \\ \sigma(t) v_{\text{ref}}(t) \cos e_3(t) \\ 0 \\ -\dot{a}_l(t) \\ -\dot{a}_r(t) \end{pmatrix}$$

with $v_c(t)$ and $\omega_c(t)$ given by (12), and $e_1(t)$, $e_2(t)$, and $e_3(t)$ given by (10).

Note that the perturbation term $g(t, e_a(t))$ vanishes at the origin $e_a(t) = 0$. However, since the parameters $\sigma(t)$, $\dot{a}_l(t)$, and $\dot{a}_r(t)$ can be nonzero, the perturbation term $g_n(t, 0)$ in general does not vanish at the origin. This implies that the origin $e_a(t) = 0$ might not be an equilibrium point of the system (25). Consequently, it is no longer possible to analyze the stability of the origin $e_a(t) = 0$ as an equilibrium point of the system (25), nor should it be expected that $e_a(t)$ will converge to zero with $t \rightarrow \infty$. However, it is still possible to study the ultimate boundedness of the solution $e_a(t)$ of the perturbed system (25). For this purpose, and to make the analysis tractable, the following set of assumptions will be used:

Assumption 1. The parameters b , k_1 , k_2 , k_3 , γ_1 , and γ_2 are all finite positive constants. Furthermore:

- (1) $v_{\text{ref}}(t)$, $\omega_{\text{ref}}(t)$, $a_l(t)$ and $a_r(t)$ are continuously differentiable, and $\sigma(t)$ is piecewise continuous in time.
- (2) $a_l(t) \geq 1$, $a_r(t) \geq 1$, $v_{\text{ref}}(t) \geq \mu_1 > 0$, and $|2v_{\text{ref}}(t) \pm b\omega_{\text{ref}}(t)| \geq \mu_2 > 0$ for some $\mu_1 > 0$ and $\mu_2 > 0$.
- (3) $v_{\text{ref}}(t)$, $\omega_{\text{ref}}(t)$, $a_l(t)$, $a_r(t)$, and $\sigma(t)$ are bounded on $[0, \infty)$.
- (4) $\dot{v}_{\text{ref}}(t)$, $\dot{\omega}_{\text{ref}}(t)$, $\dot{a}_l(t)$, $\dot{a}_r(t)$, and $\sigma(t)$ can be made arbitrarily small.

The next theorem presents our main result.

Theorem 3.1. *Under Assumption 1, the solution $e_a(t)$ of (25) is uniformly ultimately bounded, for sufficiently small positive scalars γ_1 and γ_2 . Thus, there exist positive*

constants α , u_b , T such that

$$\|e_a(t)\| \leq \alpha \exp[-\gamma(t - t_0)] \|e_a(t_0)\|, \quad \forall t_0 \leq t < t_0 + T$$

and

$$\|e_a(t)\| \leq u_b, \quad \forall t \geq t_0 + T$$

The proof of Theorem 3.1 will be pursued in two steps. First, it is shown in Section 3.4 that the origin $e_a(t) = 0$ of the nominal system

$$\dot{e}_a = f_a(t, e_a(t)) \tag{26}$$

is exponentially stable if the derivatives of $v_{\text{ref}}(t)$, $\omega_{\text{ref}}(t)$, $a_l(t)$ and $a_r(t)$ are sufficiently small, that is, as long as those parameters vary slowly. Second, it is shown in Section 3.5 that the origin $e_a(t) = 0$ of the system

$$\dot{e}_a(t) = f_a(t, e_a(t)) + g(t, e_a(t)) \tag{27}$$

is also exponentially stable, which allows us to conclude that the solution $e_a(t)$ of the perturbed system (25) is ultimately bounded as long as the lateral slip $\sigma(t)$ remains small.

3.4. Exponential stability of the nominal system

It will now be shown that the origin $e_a = 0$ of the nonlinear nominal system (26) is exponentially stable using Theorem A.3, given in Appendix A. This theorem allows us to assert exponential stability of the origin of (26) based on the exponential stability of the origin of the linear time-varying

$$\dot{e}(t) = A(t)e(t) \tag{28}$$

with $A(t)$ the Jacobian of $f_a(t, e_a)$ evaluated at $e_a = 0$. The matrix $A(t)$ is given by

$$A(t) = \begin{pmatrix} A_{11}(t) & A_{12}(t) \\ A_{21}(t) & A_{22}(t) \end{pmatrix} \tag{29}$$

where

$$\begin{aligned}
A_{11}(t) &= \begin{pmatrix} -k_1 & \omega_{\text{ref}}(t) & k_3\omega_{\text{ref}}(t) \\ -\omega_{\text{ref}}(t) & 0 & v_{\text{ref}}(t) \\ 0 & -\frac{k_2}{2}v_{\text{ref}}(t) & -\frac{k_4}{2k_3}v_{\text{ref}}(t) \end{pmatrix} \\
A_{12}(t) &= \frac{1}{4ba_l(t)a_r(t)} \begin{pmatrix} ba_r(t)v_2(t) & -ba_l(t)v_1(t) \\ 0 & 0 \\ -2a_r(t)v_2(t) & -2a_l(t)v_1(t) \end{pmatrix} \\
A_{21}(t) &= \frac{1}{4bk_2} \begin{pmatrix} -bk_2\gamma_1v_2(t) & 2k_2k_3\gamma_1v_2(t) & 2\gamma_1k_4v_2(t) \\ bk_2\gamma_2v_1(t) & 2k_2k_3\gamma_2v_1(t) & 2\gamma_2k_4v_1(t) \end{pmatrix} \\
A_{22}(t) &= \begin{pmatrix} 0 & 0 \\ 0 & 0 \end{pmatrix}
\end{aligned}$$

with $v_1(t) = b\omega_{\text{ref}}(t) + 2v_{\text{ref}}(t)$, $v_2(t) = b\omega_{\text{ref}}(t) - 2v_{\text{ref}}(t)$, and $k_4 = 1 + k_2k_3^2$.

The next Remark gathers all conditions on $f_a(t, e_a)$ and its Jacobian matrix required by Theorems A.3 and A.4, given in Appendix A.

Remark 2. When Assumption 1 holds, $f_a(t, e_a)$ defined in (25) is continuously differentiable, and $f_a(t, 0)$ is uniformly bounded for all $t \geq 0$. Moreover, the Jacobian matrix $J(t, e_a) = \partial f_a(t, e_a) / \partial e_a$ is bounded and Lipschitz in e_a , uniformly in t , matrix $A(t) = J(t, 0)$, given by (29), is elementwise bounded and differentiable, and the derivative $\dot{A}(t)$ can be made arbitrarily small.

It now remains to show that the origin of the linear time-varying system (28) is exponentially stable. This can be accomplished using Theorem A.4, which asserts the stability of “slowly varying” systems from the stability properties of the frozen-time systems, i.e., from the eigenvalues of $A(t)$. The proof that the eigenvalues of $A(t)$ satisfy the requirement of Theorem A.4 is the context of the next result.

Proposition 3.2. *Let $A(t)$ be given by (29). Then, under Assumption 1, there exists a scalar $\epsilon > 0$ such that*

$$\text{Re}[\lambda(A(t))] \leq -\epsilon < 0$$

for sufficiently small positive scalars γ_1 and γ_2 .

Proof. Consider the characteristic polynomial of matrix $A(t)$, which is given by

$$p(s) = s^5 + \alpha_1(t)s^4 + \alpha_2(t)s^3 + \alpha_3(t)s^2 + \alpha_4(t)s + \alpha_5(t), \quad (30)$$

whose coefficients $\alpha_i(t)$ are given in Appendix C. Under Assumption 1, it is clear there exists a $\delta_1 > 0$ such that $\alpha_i(t) \geq \delta_1$, for $i = 1, \dots, 5$.

The second form of the stability criterion of Liénard and Chipart (Gantmacher, 1959), given in Appendix B, establishes the necessary and sufficient conditions for all the roots of the real polynomial $p(s)$, given by (30), to have negative real parts. These conditions are given by

- (1) $\alpha_1(t) > 0$, $\alpha_3(t) > 0$, and $\alpha_5(t) > 0$;
- (2) $0 < c_2(t) := \alpha_1(t)\alpha_2(t) - \alpha_3(t)$;
- (3) $0 < c_3(t) := (\alpha_1(t)\alpha_2(t) - \alpha_3(t))(\alpha_3(t)\alpha_4(t) - \alpha_2(t)\alpha_5(t)) - (\alpha_1(t)\alpha_4(t) - \alpha_5(t))^2$.

Since it is already known that $0 < \delta_1 \leq \alpha_i(t)$, for $i = 1, \dots, 5$, the first condition is satisfied, and the second condition holds true by noticing that the expression

$$\begin{aligned}
c_2(t) &= \alpha_1(t)\alpha_2(t) - \alpha_3(t) \\
&= \frac{1}{16a_l(t)a_r(t)b^2k_2k_3^2} \left\{ a_l(t) \left[4a_r(t)b^2k_2 \left(k_1(k_4^2v_{\text{ref}}^2(t) + 4k_3^2\omega_{\text{ref}}^2(t)) \right. \right. \right. \\
&\quad \left. \left. \left. + 2k_1^2k_3k_4v_{\text{ref}}(t) + k_2k_3v_{\text{ref}}(t)(k_4v_{\text{ref}}^2(t) + 2k_3^2\omega_{\text{ref}}^2(t)) \right) \right] \right. \\
&\quad \left. + \gamma_2k_3v_1^2(t) (b^2k_1k_2k_3 + 2(k_2^2k_3^4v_{\text{ref}}(t) + v_{\text{ref}}(t))) \right] \\
&\quad \left. + a_r(t)\gamma_1k_3v_2^2(t) (b^2k_1k_2k_3 + 2(k_2^2k_3^4v_{\text{ref}}(t) + v_{\text{ref}}(t))) \right\} \\
&> \frac{k_1^2k_4v_{\text{ref}}(t)}{2k_3} \geq v_{\text{ref}}(t)k_1^2\sqrt{k_2} \geq \mu_1k_1^2\sqrt{k_2} > 0
\end{aligned}$$

is positive.

It now remains to show the third condition. For that purpose, first notice that the expression for $c_3(t)$ can be rearranged as

$$c_3(t) = c_2(t)\alpha_3(t)\alpha_4(t) - \rho(t), \quad \rho(t) = \alpha_1^2(t)\alpha_4^2(t) + \alpha_5(t)(c_2(t)\alpha_2(t) - 2\alpha_1(t)\alpha_4(t) + \alpha_5(t)) \quad (31)$$

and that $\alpha_3(t)$ is bounded below by

$$\alpha_3(t) \geq v_{\text{ref}}^2(t)k_2k_1/2$$

This last inequality directly implies that

$$c_2(t)\alpha_3(t) = \alpha_1(t)\alpha_2(t)\alpha_3(t) - \alpha_3^2(t) \geq v_{\text{ref}}^3(t)k_1^3\sqrt{k_2^3}/2 \geq \delta_2 > 0, \quad \text{with } \delta_2 = \mu_1^3k_1^3\sqrt{k_2^3}/2$$

Notice also that $c_2(t)\alpha_3(t)\alpha_4(t)$ is bounded below as follows

$$c_2(t)\alpha_3(t)\alpha_4(t) \geq \frac{k_1k_3\mu_1\mu_2^2\delta_2}{4b^2\mathcal{A}}\gamma_1 + \frac{k_1k_3\mu_1\mu_2^2\delta_2}{4b^2\mathcal{A}}\gamma_2 + \frac{k_4\mu_2^4\delta_2}{16b^2k_2\mathcal{A}^2}\gamma_1\gamma_2 > 0 \quad (32)$$

where $\mathcal{A} = \sup \{a_l(t), a_r(t)\}$ is finite by Assumption 1. Likewise, the term $\rho(t)$ in (31) can also be written as a polynomial expression in γ_1 and γ_2 as follows

$$\rho(t) = p_{11}(t)\gamma_1\gamma_2 + p_{20}(t)\gamma_1^2 + p_{02}(t)\gamma_2^2 + p_{21}(t)\gamma_1^2\gamma_2 + p_{12}(t)\gamma_1\gamma_2^2 + \dots \quad (33)$$

where the coefficients $p_{ij}(t)$ are bounded by Assumption 1. Thus, for sufficiently small γ_1 and γ_2 , the first two terms on the right-hand side of (32) dominate all the remaining terms in the expression for $c_3(t)$ given by (31), and hence there is a $\delta_3 > 0$ such that $c_3(t) \geq \delta_3$ for all $t \geq 0$.

This concludes our proof and it has been shown (see Theorem B.1 and Remark 3 in Appendix B) that $\text{Re}[\lambda_j(A(t))] \leq -\epsilon < 0$. □

Therefore, from Proposition 3.2, all conditions of Theorem A.4 have been satisfied, which means there is some $\epsilon_d > 0$ such that if $|\dot{a}_{ij}| \leq \epsilon_d$, the origin $e_a(t) = 0$ of the linear time-varying system (28) is exponentially stable. From (29), it is readily

seen that, for arbitrarily small $\epsilon_d > 0$, if $\dot{v}_{\text{ref}}(t)$, $\dot{\omega}_{\text{ref}}(t)$, $\dot{a}_r(t)$, and $\dot{a}_l(t)$ are bounded by sufficiently small values, it is possible to enforce $|\dot{a}_{ij}(t)| \leq \epsilon_d$. In this case, the origin $e_a = 0$ of the linear time-varying system (28) is exponentially stable and, from Theorem A.3, the origin $e_a(t) = 0$ of the nonlinear system (26) is also exponentially stable.

3.5. Ultimate boundedness of solutions of the perturbed system

Since the origin $e_a(t) = 0$ of the nominal system (26) has been shown to be exponentially stable, under Assumption 1, Lemma A.1 (given in Appendix A) is applied to show that the origin $e_a(t) = 0$ of the perturbed system (27) is also exponentially stable. By exponential stability of the origin, the existence of a Lyapunov function for the nominal system (26) that satisfies conditions (A3)-(A5) is ensured by a Lyapunov converse theorem (see, for instance, Theorem 4.14 from Khalil (2002)), provided that $\partial f/\partial e_a$ is bounded on a domain $D = \{e_a \in \mathbb{R}^5 \mid \|e_a(t)\| < d\}$, uniformly in t . This is indeed the case, since $f_a(t, e_a)$ is composed of polynomial and sinusoidal functions of e_a and continuous time-varying functions that are bounded for all $t \geq 0$. To successfully conclude the application of Lemma A.1, it remains to show that conditions (A6) and (A7) are satisfied. To verify this, first write $g(t, e_a) = \sigma(t)\bar{g}(t, e_a)$. The vector function $\bar{g}(t, e_a)$ is continuously differentiable in e_a , and thus $\|\partial\bar{g}/\partial e_a\| \leq \bar{b}$ on $[0, \infty) \times D$ for some $\bar{b} > 0$ (the bound b is independent of t , due to Assumption 1). Thus $\bar{g}(t, e_a)$ is Lipschitz in e_a on the compact domain D , uniformly in t , with Lipschitz constant \bar{b} (see, for instance, (Khalil, 2002, Lemma 3.1)). Since $\bar{g}(t, 0) = 0$ and $\bar{g}(t, e_a)$ is Lipschitz in e_a , it follows that $\|g(t, e_a)\| \leq |\sigma(t)|\bar{b}\|e_a\|$, and condition (A6) is verified; this also implies that, for a sufficiently small bound on $|\sigma(t)|$, condition (A7) is verified. Thus, the origin of the nominal system perturbed by the vanishing term, given by (27), is also exponentially stable, provided that the magnitude of the lateral slip is bounded by a sufficiently small value.

Since the origin $e_a(t) = 0$ is an exponentially stable equilibrium point of the system (27), Lemma A.2 (given in Appendix A) can be applied to show that the solution $e_a(t)$ of the perturbed system (25) is ultimately bounded by a small bound. For this purpose, the perturbed system (25) is rewritten as

$$\dot{e}_a = f(t, e_a) + g_n(t, e_a)$$

with $f(t, e_a) = f_a(t, e_a) + g(t, e_a)$. To use Lemma A.2, it is necessary to find a Lyapunov function $V(t, e_a(t))$ for the system (27) that satisfies the conditions (A3), (A4), and (A5). This Lyapunov function indeed exists, since the Lyapunov function for the system (26) is also a Lyapunov function for the system (27). This fact is shown in the proof of Lemma A.1 in Khalil (2002). To conclude the application of Lemma A.2, it remains to show that condition (A8) is satisfied. The proof of this fact uses exactly the same reasoning used to prove that conditions (A6) and (A7) are satisfied. This concludes the proof of Theorem 3.1.

4. Numerical results

This section presents some numerical simulations of the proposed adaptive control strategy given in Section 3. These simulations aim to provide an illustration of our theoretical results, and give an idea of the performance of the adaptive kinematic

controller (AKC) whose block diagram is shown in Figure 2. To illustrate how adaptation affects performance, the non-adaptive kinematic controller (NKC) given by (12) will also be simulated, as it can be viewed as a version of the adaptive scheme where adaptation is “turned off”.

In all simulations, the physical parameters of the wheeled robot model, taken from Ryu and Agrawal (2011), are given by $b = 0.1624$ m and $r = 0.0825$ m. The reference trajectory used in the simulations is also fixed, and is described in Appendix D. Fixing the reference trajectory in this numerical analysis is justified by the fact that, in many applications, the robot must follow a specific planned trajectory. Figure 3 shows the reference trajectory $(x_{\text{ref}}(t), y_{\text{ref}}(t))$ generated using the input $\eta_{\text{ref}}(t) = (v_{\text{ref}}(t), \omega_{\text{ref}}(t))^T$. Note that the reference trajectory can be divided in three parts. The first part consists of a straight line path that occurs on the interval $0 \text{ s} \leq t < 25 \text{ s}$, the second part consists of a curved path with time-varying radius of curvature that occurs on the interval $25 \text{ s} \leq t < 45 \text{ s}$, and the third part consists of a straight line path that occurs on the interval $t \geq 45 \text{ s}$.

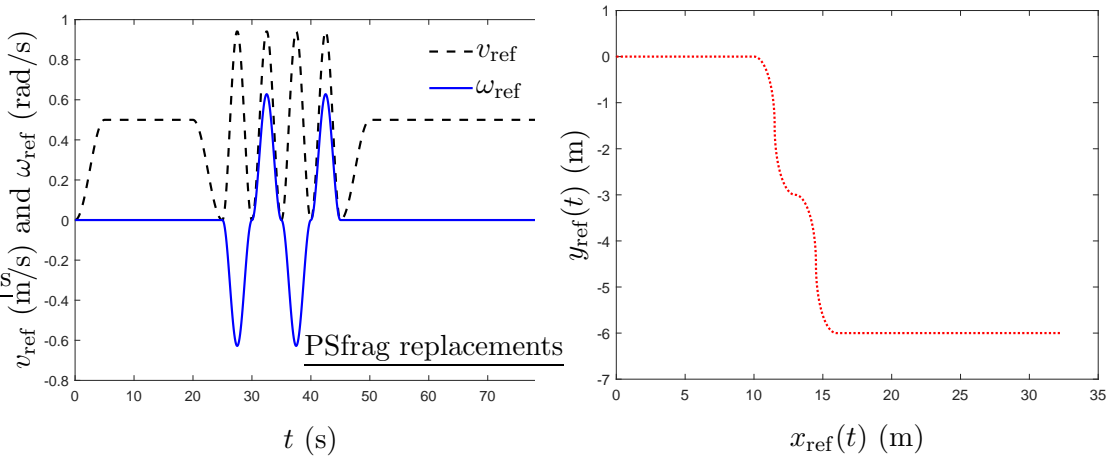


Figure 3. Reference trajectory $(x_{\text{ref}}(t), y_{\text{ref}}(t))$ generated by the reference input $\eta_{\text{ref}}(t) = (v_{\text{ref}}(t), \omega_{\text{ref}}(t))^T$.

To simulate the controlled robot, it is also necessary to select the controller gains. A standard criterion for choosing optimal controller gains involves minimizing the cost function given by

$$\mathcal{F} = \int_0^{t_f} e^T Q e + (\xi - \xi_{\text{ref}})^T R (\xi - \xi_{\text{ref}}) dt$$

with $Q > 0$ and $R \geq 0$, which represents weights energy of states and control actions spent while the robot is moving. This criterion is adopted to select gains for both the NKC and AKC schemes, using $Q = I$ and $R = 0.05I$. Notice that the term $\xi - \xi_{\text{ref}}$ represents the difference between the controlled wheel speeds and the reference wheel speeds resulting from the reference trajectory η_{ref} . This difference depends on the longitudinal slip parameters $a_l(t)$ and $a_r(t)$, which also need to be provided so that \mathcal{F} can be minimized. Since the NKC is not designed to take into account the slip, for the purposes of gain selection, the robot controlled by the NKC is subjected to zero slip. Thus, for the NKC, $\xi - \xi_{\text{ref}} = \Phi_0^{-1}(\eta_c(t) - \eta_{\text{ref}})$, where Φ_0 denotes the matrix (6) with $a_l = a_r = 1$. The AKC, on the other hand, has to be able to deal with the

slip. For this reason, to select the gains for the AKC, a “training” slip profile given by $a_l(t) = 5/3(H(t - 15) - H(t - 50))$ and $a_r(t) = 5/2(H(t - 30) - H(t - 65))$ is used, where $H(\cdot)$ denotes the Heaviside step function. Using this slip, the controlled and reference wheel speeds for the AKC are given by $\xi = \hat{\Phi}(t)^{-1}\eta_c(t)$ and $\xi_{\text{ref}} = \Phi(t)^{-1}\eta_{\text{ref}}$, respectively.

To select controller gains for the NKC and AKC schemes, a grid search over the gains k_i ($i = 1, 2, 3$) was performed, and those gains that yielded the smallest \mathcal{F} were selected. The grid was chosen such that k_1 , k_2 and k_3 range over 20 equally spaced points in logarithmic scale between 10^{-1} and 10 . For the AKC scheme, the values $\gamma_1 = \gamma_2 = 3$ were fixed a priori. The minimum value of \mathcal{F} using the AKC scheme is indicated in Figure 4(a) by a circle, and was obtained when $(k_1, k_2, k_3) = (1.44, 10, 1.83)$. Using the NKC scheme, the gains $(k_1, k_2, k_3) = (0.26, 10, 0.1)$ provided the smallest value for \mathcal{F} , as indicated in Figure 4(b). The set of gains that provided a minimum \mathcal{F} using each controller will be called henceforth the best-known gains.

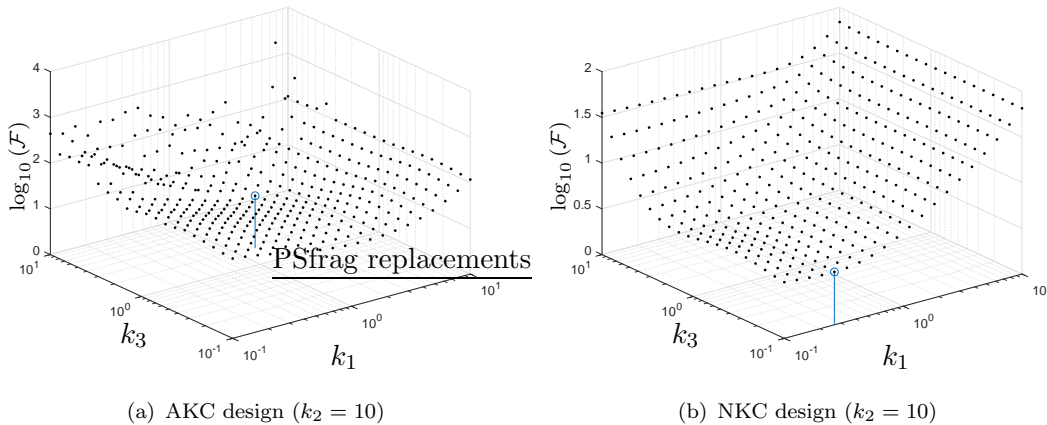


Figure 4. Value of \mathcal{F} for k_1 and k_3 for the fixed value $k_2 = 10$.

Once the controller gains have been selected, to verify the performance of the NKC and AKC schemes, the robot under both schemes is subjected to a “validation” slip profile, which is a more challenging slip profile, chosen so as to vary significantly in time. The longitudinal slip parameters $a_l(t)$ and $a_r(t)$ and the lateral slip parameter $\sigma(t)$ are chosen as the following nonlinear time-varying signals

$$\begin{aligned} a_l(t) &= 1 / (0.7 + 0.3 \exp(-0.1t) \cos(1.1t)) \\ a_r(t) &= 1 / (0.4 + 0.6 \exp(-0.08t) \sin^2(0.02t^2)) \\ \sigma(t) &= 3.0 \exp(-0.03t) \text{sinc}(t - 35.0) \end{aligned}$$

Figure 5 shows the longitudinal slip parameters $a_l(t)$ and $a_r(t)$ and the lateral slip parameter $\sigma(t)$. Physically, it is expected that a high variation of the longitudinal slip will occur when the robot is accelerating. This occurs, for example, when the robot starts its motion from rest. It is also expected that a high variation of the lateral slip will occur when the robot moves along a curve. Note that a high value of the lateral slip occurs in the middle of the interval $25 \text{ s} \leq t < 45 \text{ s}$, where the reference trajectory is a curved path. It is well known that the lateral slip is zero during straight line motion. However, different values of longitudinal slip may cause small lateral slip.

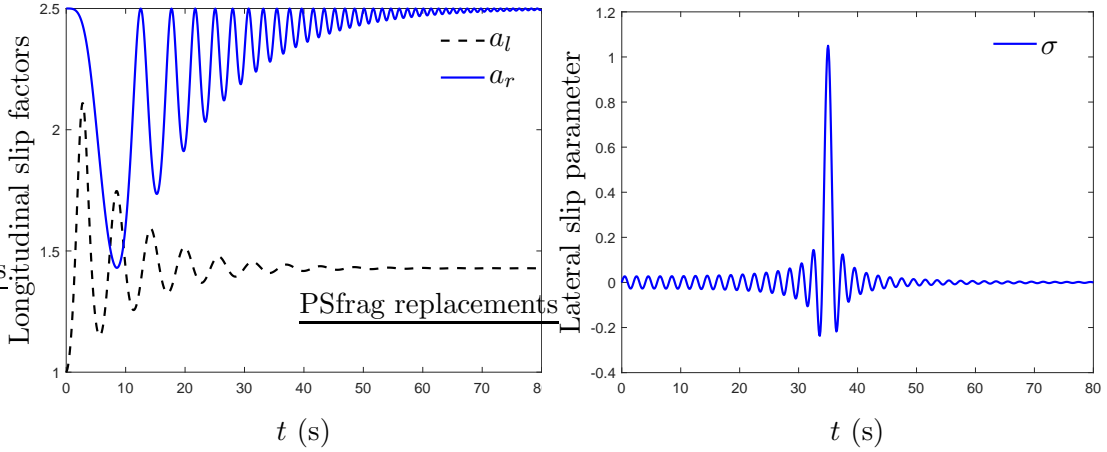


Figure 5. Longitudinal slip parameters $a_l(t)$ and $a_r(t)$ and lateral slip parameter $\sigma(t)$.

Figures 6 through 9 show the simulations using the AKC and NKC schemes with the best-known gains. Figure 6 shows the robot trajectory obtained using the NKC and AKC schemes. The dotted line, the dashed line and the solid line stand, respectively, for the reference trajectory, the robot trajectory obtained using the NKC scheme, and the robot trajectory obtained using the AKC scheme. The initial condition of the robot, indicated by a black circle, is $q_p(0) = (1/2, -3/4, -\pi/6)^T$. Note that the robot with the AKC scheme is able to follow the reference trajectory with a small error. On the other hand, the NKC scheme is not able to compensate for the slip, and consequently, the robot trajectory diverges with respect to the reference trajectory.

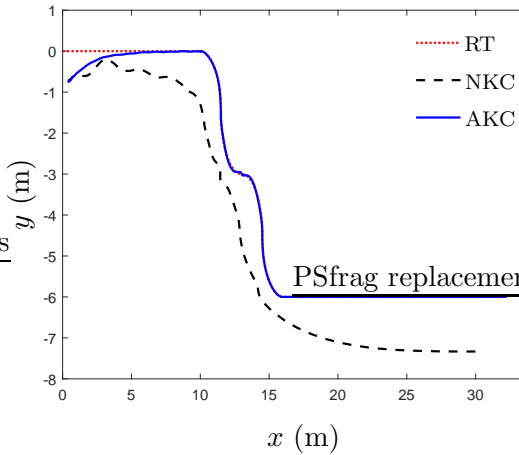


Figure 6. Reference trajectory (RT) and robot trajectory using the NKC and AKC schemes.

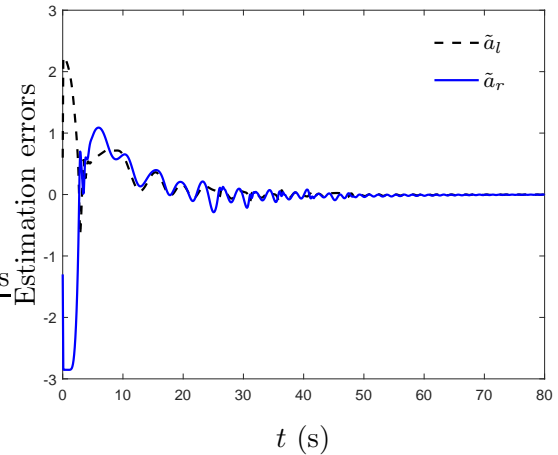


Figure 7. Estimation errors \tilde{a}_l and \tilde{a}_r .

Figure 7 shows the estimation errors \tilde{a}_l (dashed) and \tilde{a}_r (solid). The initial conditions of the update rule were taken as $\hat{a}_l(0) = 1.6$ and $\hat{a}_r(0) = 1.2$, which differ from the true values $a_l(0) = 1$ e $a_r(0) = 2.5$. Note that an estimation error occurs at the beginning of the trajectory. However, this is not surprising, since convergence is only guaranteed for constant slip parameters.

Figure 8 shows the pose error $e = (e_1, e_2, e_3)^T$. The dashed line stands for the NKC scheme, and the solid line stands for the AKC scheme. As expected, the AKC scheme

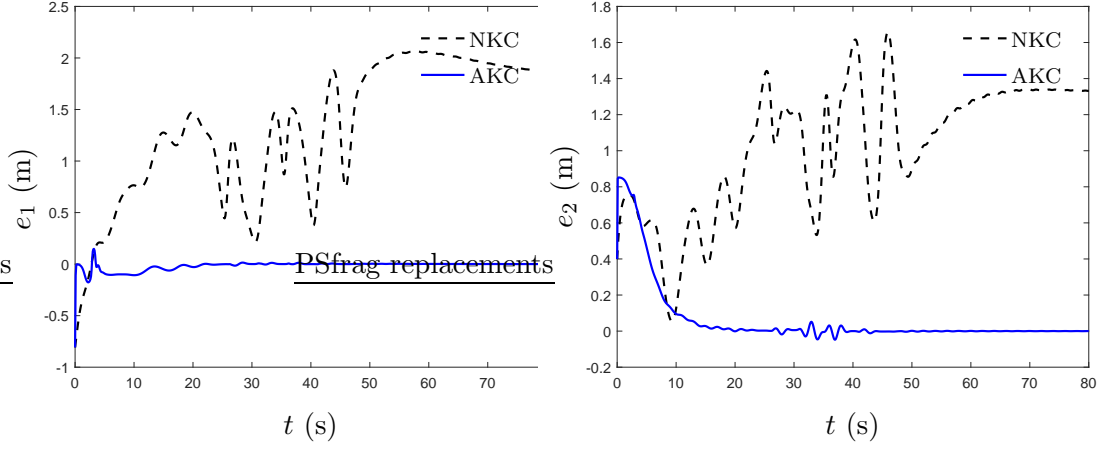


Figure 8. Pose errors e_1 and e_2 for the NKC and AKC schemes.

achieves a significantly better performance compared to the NKC scheme. Since the lateral slip $\sigma(t)$ and the longitudinal slip derivatives $\dot{a}_l(t)$ and $\dot{a}_r(t)$ tend to zero on the interval $t \geq 45$ s, the errors e_1 , e_2 and e_3 tend to zero.

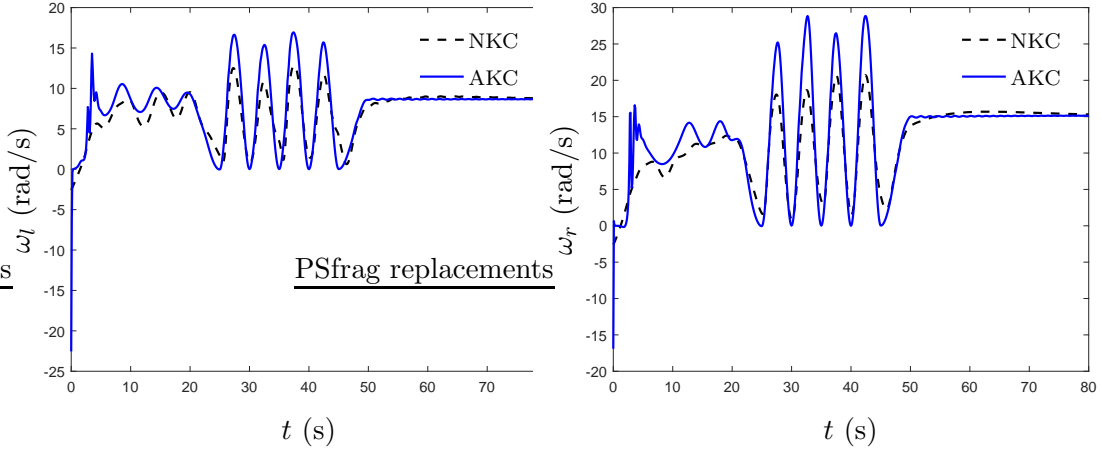


Figure 9. The angular velocity of the left wheel $\omega_l(t)$ and the angular velocity of the right wheel $\omega_r(t)$ using the NKC and AKC schemes.

Figure 9 shows the effective control input $\xi(t) = (\omega_l(t), \omega_r(t))^T$ generated by the NKC and AKC schemes. The dashed line stands for the NKC scheme, and the solid line stands for the AKC scheme. Since, for the AKC scheme, the auxiliary control input $\eta_c(t)$ converges to the reference input $\eta_{\text{ref}}(t)$, the amplitude of the effective control input $\xi(t)$ is ultimately determined by the amplitude of the reference input $\eta_{\text{ref}}(t)$.

5. Conclusions

This paper provides a nonlinear kinematic controller that guarantees reference tracking for a nonholonomic wheeled mobile robot subject to wheel slip, using only the robot pose. The paper introduces the design by defining the dynamics of the pose error including both longitudinal and lateral slip. The proposed design builds on a kinematic control law which is known to provide global trajectory tracking for wheeled mobile robots in the absence of slip. Furthermore, this design is extended to include an adap-

tive control law that compensates for the slip. Our controller is guaranteed to provide asymptotic convergence of the tracking error under time-varying references, when the robot is only subject to constant longitudinal slip.

Moreover, it is rigorously shown that the tracking error and the longitudinal slip estimation error are ultimately bounded provided that the reference trajectory and longitudinal slip are slowly varying, and the lateral slip is sufficiently small. To prove convergence of the tracking error, the error dynamics is decomposed as the sum of a nonlinear nominal term plus vanishing and nonvanishing perturbation terms. Exponential stability of the nonlinear nominal system is proved by applying stability criteria for slow time-varying linear systems to the linearized model. Subsequently, the stability under the presence of the perturbation terms are analyzed. Numerical simulations show the effectiveness of the proposed approach.

Disclosure statement

The authors declare that they have no conflict of interest.

Funding

This work was supported by the Brazilian funding agencies CAPES (Finance Code 001) and CNPq (Grant Numbers 503343/2012-9 and 311842/2013-5).

References

- Chen, M. (2017). Disturbance attenuation tracking control for wheeled mobile robots with skidding and slipping. *IEEE Transactions on Industrial Electronics*, *64*(4), 3359–3368.
- Cui, M., Huang, R., Liu, H., Liu, X., & Sun, D. (2014). Adaptive tracking control of wheeled mobile robots with unknown longitudinal and lateral slipping parameters. *Nonlinear Dynamics*, *78*, 1811–1826.
- Fierro, R., & Lewis, F. L. (1997). Control of a nonholonomic mobile robot: Backstepping kinematics into dynamics. *Journal of Robotic Systems*, *14*(3), 149–163.
- Fukao, T., Nakagawa, H., & Adachi, N. (2000). Adaptive tracking control of a nonholonomic mobile robot. *IEEE Transactions on Robotics and Automation*, *16*(5), 609–615.
- Gantmacher, F. R. (1959). *The theory of matrices* (Vol. II). New York, N.Y.: Chelsea Publishing Company.
- Gao, H., Song, X., Ding, L., Xia, K., Li, N., & Deng, Z. (2014). Adaptive motion control of wheeled mobile robot with unknown slippage. *International Journal of Control*, *87*(8), 1513–1522.
- Gonzales, R., Fiacchini, M., Alamo, T., Guzmán, J. L., & Rodriguez, F. (2009). Adaptive control for a mobile robot under slip conditions using LMI-based approach. In *Proceedings of the european control conference* (pp. 1251–1256). Budapest, Hungary.
- Ibrahim, F., Abouelsoud, A. A., Elbab, A. M. R. F., & Ogata, T. (2019). Path following algorithm for skid-steering mobile robot based on adaptive discontinuous posture control. *Autonomous Robot*, *33*(9), 439–453.
- Iossaqui, J. G., & Camino, J. F. (2013, July). Wheeled robot slip compensation for trajectory tracking control problem with time-varying reference input. In *Proceedings of the 9th international workshop on robot motion and control* (pp. 167–173). Wasowo, Poland.

- Iossaqui, J. G., Camino, J. F., & Zampieri, D. E. (2011, September). A nonlinear control design for tracked robots with longitudinal slip. In *Proceedings of the 18th ifac world congress* (pp. 5932–5937). Milano, Italy.
- Jarzebowska, E. M. (2008). Advanced programmed motion tracking control of nonholonomic mechanical systems. *IEEE Transactions on Robotics*, *24*(6), 1315–1328.
- Kanayama, Y., Kimura, Y., Miyazaki, F., & Noguchi, T. (1990). A stable tracking control method for an autonomous mobile robot. In *IEEE international conference on robotics and automation* (pp. 384–389). Cincinnati, USA.
- Khalil, H. K. (2002). *Nonlinear systems*. Upper Saddle River, USA: Prentice-Hall.
- Kim, D.-H., & Oh, J.-H. (1998). Globally asymptotically stable tracking control of mobile robots. In *Proceedings of the IEEE international conference on control applications* (pp. 1297–1301). Trieste, Italy.
- Klancar, G., Zdesar, A., Blazic, S., & Skrjanc, I. (2017). *Wheeled mobile robotics: from fundamentals towards autonomous systems*. Oxford, UK: Butterworth-Heinemann.
- Li, X., Wang, Z., Chen, X., Zhu, J., & Chen, Q. (2016). Adaptive control of unicycle-type mobile robots with longitudinal slippage. In *Proceedings of the american control conference*. Boston, MA, United States.
- Michalek, M., Dutkiewicz, P., Kielczewski, M., & Pazderski, D. (2009). Trajectory tracking for a mobile robot with skid-slip compensation in the vector-field-orientation control system. *International Journal of Applied Mathematics and Computer Science*, *19*(4), 547–559.
- Moosavian, S. A. A., & Kalantari, A. (2008). Experimental slip estimation for exact kinematics modeling and control of a tracked mobile robot. In *Proceedings of the IEEE/RSJ international conference on intelligent robots and systems* (pp. 95–100). Nice, France.
- Morin, P., & Samson, C. (2006). *Chapter trajectory tracking for non-holonomic vehicles, in lecture notes in control and information sciences*. New York, USA: Springer-Verlag.
- Nourbakhsh, I. R., & Siegwart, R. (2004). *Introduction to autonomous mobile robots*. London, UK: The MIT Press.
- Panahandeh, P., Alipour, K., Tarvirdizadeh, B., & Hadi, A. (2019). A kinematic lyapunov-based controller to posture stabilization of wheeled mobile robots. *Mechanical Systems and Signal Processing*, *134*, 1–19.
- Rosenbrock, H. H. (1963). The stability of linear time-dependent control systems. *Journal of Electronics and Control*, *15*(1), 73–80.
- Ryu, J.-C., & Agrawal, S. K. (2010, December). Differential flatness-based robust control of mobile robots in the presence of slip. *The International Journal of Robotics Research*.
- Ryu, J.-C., & Agrawal, S. K. (2011). Differential flatness-based robust control of mobile robots in the presence of slip. *The International Journal of Robotics Research*, *30*(4), 463–475.
- Shafiei, M. H., & Monfared, F. (2019). Design of a robust tracking controller for a nonholonomic mobile robot with side slipping based on lyapunov redesign and nonlinear h-infinity methods. *Systems Science & Control Engineering*, *7*(1), 1–11.
- Sidek, N., & Sarkar, N. (2008). Dynamic modeling and control of nonholonomic mobile robot with lateral slip. In *Proceedings of the 7th wseas international conference on signal processing, robotics and automation* (pp. 66–74). Cambridge, UK.
- Thomas, M., Bandyopadhyay, B., & Vachhani, L. (2019). Finite-time posture stabilization of the unicycle mobile robot using only position information: A discrete-time sliding mode approach. *International Journal of Robust and Nonlinear Control*, *29*(6), 1990–2006.
- Urakubo, T. (2015). Feedback stabilization of a nonholonomic system with potential fields: application to a two-wheeled mobile robot among obstacles. *Nonlinear Dynamics*, *81*, 1475–1487.
- Wang, D., & Low, C. B. (2008). Modeling and analysis of skidding and slipping in wheeled mobile robots: Control design perspective. *IEEE Transactions on Robotics*, *24*(3), 676–687.
- Ward, C. C., & Iagnemma, K. (2008). A dynamic-model-based wheel slip detector for mobile robots on outdoor terrain. *IEEE Transactions on Robotics*, *24*(4), 821–831.
- Wu, J., Xu, G., & Yin, Z. (2009). Robust adaptive control for a nonholonomic mobile robot with unknown parameters. *Journal of Control Theory and Applications*, *7*(2), 212–218.

- Zhai, J.-Y., & Song, Z.-B. (2019). Adaptive sliding mode trajectory tracking control for wheeled mobile robots. *International Journal of Control*, 92(10), 2255–2262.
- Zhou, B., Peng, Y., & Han, J. (2007). UKF based estimation and tracking control of non-holonomic mobile robots with slipping. In *IEEE international conference on robotics and biomimetics* (pp. 2058–2063). Sanya, China.

Appendix A. Supporting results

A.1. Ultimate boundedness

Consider the system

$$\dot{x}(t) = f(t, x(t)) + g(t, x(t)) \quad (\text{A1})$$

where $f : [0, \infty) \times D \rightarrow \mathbb{R}^n$ and $g : [0, \infty) \times D \rightarrow \mathbb{R}^n$ are piecewise continuous in t and locally Lipschitz in x on $[0, \infty) \times D$, and $D \subset \mathbb{R}^n$ is a domain that contains the origin $x = 0$. Consider system (A1) as a perturbation of the nominal system

$$\dot{x}(t) = f(t, x(t)) \quad (\text{A2})$$

Suppose $x = 0$ is an exponentially stable equilibrium point of the nominal system (A2), and let $V(t, x(t))$ be a Lyapunov function that satisfies

$$c_1 \|x(t)\|^2 \leq V(t, x(t)) \leq c_2 \|x(t)\|^2 \quad (\text{A3})$$

$$\frac{\partial V(t, x(t))}{\partial t} + \frac{\partial V(t, x(t))}{\partial x(t)} f(t, x(t)) \leq -c_3 \|x(t)\|^2 \quad (\text{A4})$$

$$\left\| \frac{\partial V(t, x(t))}{\partial x(t)} \right\| \leq c_4 \|x(t)\| \quad (\text{A5})$$

for all $(t, x(t)) \in [0, \infty) \times D$ for some positive constants c_1 , c_2 , c_3 , and c_4 .

For a vanishing perturbation $g(t, 0) = 0$, we can show that $x = 0$ is also an exponentially stable equilibrium point of the perturbed system (A1) using the next lemma.

Lemma A.1 (Lemma 9.1 from Khalil (2002)). *Let $x = 0$ be an exponentially stable equilibrium point of the nominal system (A2). Let $V(t, x(t))$ be a Lyapunov function of the nominal system that satisfies (A3) through (A5) in $[0, \infty) \times D$. Suppose the perturbation term $g(t, x(t))$ satisfies*

$$\|g(t, x(t))\| \leq \gamma \|x(t)\|, \quad \forall t \geq 0, \quad \forall x(t) \in D \quad (\text{A6})$$

and

$$\gamma < \frac{c_3}{c_4} \quad (\text{A7})$$

Then, the origin is an exponentially stable equilibrium point of the perturbed system (A1).

For the more general case, in which it is not known whether $g(t, 0) = 0$, we can no longer study stability of the origin as an equilibrium point, nor should we expect the solution of the perturbed system to approach the origin as $t \rightarrow \infty$. However, we can show that the solution is ultimately bounded by a small bound using the next lemma.

Lemma A.2 (Lemma 9.2 from Khalil (2002)). *Let $x = 0$ be an exponentially stable equilibrium point of the nominal system (A2). Let $V(t, x(t))$ be a Lyapunov function of the nominal system that satisfies (A3) through (A5) in $[0, \infty) \times D$, where $D = \{x(t) \in \mathbb{R}^n \mid \|x(t)\| < d\}$. Suppose the perturbation term $g(t, x(t))$ satisfies*

$$\|g(t, x(t))\| \leq \delta < \frac{c_3}{c_4} \sqrt{\frac{c_1}{c_2}} \theta d \quad (\text{A8})$$

for all $t \geq 0$, all $x(t) \in D$, and some positive constant $\theta < 1$. Then, for all $\|x(t_0)\| < \sqrt{c_1/c_2}d$, the solution $x(t)$ of the perturbed system (A1) satisfies

$$\|x(t)\| \leq \alpha \exp[-\gamma(t - t_0)] \|x(t_0)\|, \quad \forall t_0 \leq t < t_0 + T$$

and

$$\|x(t)\| \leq u_b, \quad \forall t \geq t_0 + T$$

for some finite T , where

$$\alpha = \sqrt{\frac{c_2}{c_1}}, \quad \gamma = \frac{(1 - \theta)c_3}{2c_2}, \quad u_b = \frac{c_4}{c_3} \sqrt{\frac{c_2}{c_1}} \frac{\delta}{\theta}$$

A.2. Linearization

To show that the origin $x = 0$ of a nonlinear system is locally exponentially stable, the following well-know result is used:

Theorem A.3 (Theorem 4.15 from Khalil (2002)). *Let $x(t) = 0$ be an equilibrium point for the nonlinear system*

$$\dot{x}(t) = f(t, x(t))$$

where $f : [0, \infty) \times D \rightarrow \mathbb{R}^n$ is continuously differentiable, $D = \{x(t) \in \mathbb{R}^n \mid \|x(t)\|_2 < d\}$, and the Jacobian matrix $[\partial f(t, x(t))/\partial x(t)]$ is bounded and Lipschitz on D , uniformly in t . Let

$$A(t) = \left. \frac{\partial f(t, x(t))}{\partial x(t)} \right|_{x(t)=0}$$

Then, $x(t) = 0$ is an exponentially stable equilibrium point for the nonlinear system if and only if it is an exponentially stable equilibrium point for the linear system

$$\dot{x}(t) = A(t)x(t)$$

Notice that exponential stability in A.3 is uniform, see (Khalil, 2002, Definition 4.5).

To show that the origin of a linear time-varying system is exponentially stable, the next theorem can be used:

Theorem A.4 (Theorem 1 of Rosenbrock (1963)). *Let $\dot{x}(t) = A(t)x(t)$, where for all $t \geq t_0$ every element $a_{ij}(t)$ of $A(t)$ is differentiable and satisfies $|a_{ij}(t)| \leq c$ and every eigenvalue λ of $A(t)$ satisfies*

$$\operatorname{Re}[\lambda(A(t))] \leq -\epsilon < 0$$

Then, there is some $\epsilon_d > 0$ (independent of t) such that if every $|\dot{a}_{ij}| \leq \epsilon_d$, the equilibrium point $x(t) = 0$ is asymptotically stable.

Notice that although the above result, which is reproduced from Rosenbrock (1963), concludes *asymptotic* stability of the origin, the proof found in Rosenbrock (1963) shows that *exponential* stability also holds.

Appendix B. Stability criterion of Liénard and Chipart

Theorem B.1 (Theorem 11 from Gantmacher (1959)). *Necessary and sufficient conditions for all the roots of the real polynomial*

$$p(s) = \alpha_0 s^n + \alpha_1 s^{n-1} + \dots + \alpha_n \quad (\alpha_0 > 0)$$

to have negative real parts can be given in any one of the following four forms:

- (1) $\alpha_n > 0, \alpha_{n-2} > 0, \dots; \Delta_1 > 0, \Delta_3 > 0, \dots,$
- (2) $\alpha_n > 0, \alpha_{n-2} > 0, \dots; \Delta_2 > 0, \Delta_4 > 0, \dots,$
- (3) $\alpha_n > 0, \alpha_{n-1} > 0, \alpha_{n-3} > 0, \dots; \Delta_1 > 0, \Delta_3 > 0, \dots,$
- (4) $\alpha_n > 0, \alpha_{n-1} > 0, \alpha_{n-3} > 0, \dots; \Delta_2 > 0, \Delta_4 > 0, \dots,$

where

$$\Delta_i = \det \begin{bmatrix} \alpha_1 & \alpha_3 & \alpha_5 & \cdots & & \\ \alpha_0 & \alpha_2 & \alpha_4 & \cdots & & \\ 0 & \alpha_1 & \alpha_3 & \cdots & & \\ 0 & \alpha_0 & \alpha_2 & \alpha_4 & & \\ & & & & \ddots & \\ & & & & & \alpha_i \end{bmatrix} \quad (\alpha_k = 0 \text{ for } k > n)$$

is the Hurwitz determinant of order i ($i = 1, 2, \dots, n$).

Remark 3. In this paper, the main application of above Theorem B.1 is concerned with the stability of matrix $A(t)$, which is time varying. Thus, the coefficient of its characteristic polynomial

$$p(s) = sI - A(t) = \alpha_0(t)s^n + \alpha_1(t)s^{n-1} + \dots + \alpha_n(t)$$

will also be a function of time.

However, one of the coefficient $\alpha_i(t)$, although been strictly positive at any instant of time, $\alpha_i(t) > 0$, might have the property that $\lim_{t \rightarrow \infty} \alpha_i(t) = 0$, and consequently

$$\lim_{t \rightarrow \infty} \operatorname{Re}[\lambda_j(A(t))] = 0$$

for some eigenvalue λ_j . To overcome this fact in order to impose the eigenvalues are bounded away from the imaginary axis by an amount $\epsilon > 0$, such that

$$\lambda_j(A(t)) < -\epsilon < 0$$

it is necessary to impose a constant lower bound $\nu > 0$ on all the conditions in Theorem B.1. For instance, the first condition must be replaced by

$$(1) \quad \alpha_n > \nu > 0, \alpha_{n-2} > \nu > 0, \dots; \Delta_1 > \nu > 0, \Delta_3 > \nu > 0, \dots,$$

Appendix C. Characteristic polynomial

The characteristic polynomial of matrix $A(t)$, defined in (29), is

$$p(s) = s^5 + \alpha_1(t)s^4 + \alpha_2(t)s^3 + \alpha_3(t)s^2 + \alpha_4(t)s + \alpha_5(t)$$

with the coefficients $\alpha_i(t)$ given by

$$\begin{aligned} \alpha_1(t) &= k_1 + \frac{k_4}{2k_3}v_{\text{ref}} \\ \alpha_2(t) &= \frac{1}{16a_l a_r b^2 k_2 k_3} \left\{ a_l \left[\gamma_2 v_1^2 k_3 (b^2 k_2 + 4k_4) + 8a_r b^2 k_2 (v_{\text{ref}}(k_1 k_4 + k_2 k_3 v_{\text{ref}}) + 2k_3 \omega_{\text{ref}}^2) \right] \right. \\ &\quad \left. + a_r \gamma_1 v_2^2 k_3 (b^2 k_2 + 4k_4) \right\} \\ \alpha_3(t) &= \frac{1}{32a_l a_r b^2 k_2 k_3} \left\{ a_r \left[16a_l b^2 k_2 v_{\text{ref}} (k_1 k_2 k_3 v_{\text{ref}} + \omega_{\text{ref}}^2) \right. \right. \\ &\quad \left. \left. + \gamma_1 v_2^2 (k_2 v_{\text{ref}} (k_3^2 (b^2 k_2 + 8) + b^2) + 8k_1 k_3 k_4) \right] \right. \\ &\quad \left. + a_l \gamma_2 v_1^2 [k_2 v_{\text{ref}} (k_3^2 (b^2 k_2 + 8) + b^2) + 8k_1 k_3 k_4] \right\} \\ \alpha_4(t) &= \frac{1}{32a_l a_r b^2 k_2} \left\{ \gamma_2 v_1^2 \left[a_l \left((bk_2 v_{\text{ref}} + 2\omega_{\text{ref}})^2 + 4\omega_{\text{ref}}^2 + 8k_1 k_2 k_3 v_{\text{ref}} \right) + 2v_2^2 \gamma_1 k_4 \right] \right. \\ &\quad \left. + a_r \gamma_1 v_2^2 \left((bk_2 v_{\text{ref}} - 2\omega_{\text{ref}})^2 + 4\omega_{\text{ref}}^2 + 8k_1 k_2 k_3 v_{\text{ref}} \right) \right\} \\ \alpha_5(t) &= \frac{1}{16a_l a_r b^2} \gamma_1 \gamma_2 k_3 v_{\text{ref}} v_1^2 v_2^2 \end{aligned}$$

with $v_1 = b\omega_{\text{ref}} + 2v_{\text{ref}}$, $v_2 = b\omega_{\text{ref}} - 2v_{\text{ref}}$, and $k_4 = 1 + k_2 k_3^2$.

Appendix D. Reference trajectory

The reference trajectory used in the simulations is generated by the numerical integration of the kinematic model (9) with the initial condition $q_{\text{ref}}(0) = (0, 0, 0)^T$ and the reference input $\eta_{\text{ref}}(t) = (v_{\text{ref}}(t), \omega_{\text{ref}}(t))^T$, adapted from

Kanayama, Kimura, Miyazaki, and Noguchi (1990), given by

$$\begin{aligned}
0 \text{ s} \leq t < 5 \text{ s} : v_{\text{ref}}(t) &= 0.25 \left(1 - \cos \left(\frac{\pi t}{5} \right) \right) & \text{and } \omega_{\text{ref}}(t) &= 0 \\
5 \text{ s} \leq t < 20 \text{ s} : v_{\text{ref}}(t) &= 0.5 & \text{and } \omega_{\text{ref}}(t) &= 0 \\
20 \text{ s} \leq t < 25 \text{ s} : v_{\text{ref}}(t) &= 0.25 \left(1 + \cos \left(\frac{\pi t}{5} \right) \right) & \text{and } \omega_{\text{ref}}(t) &= 0 \\
25 \text{ s} \leq t < 30 \text{ s} : v_{\text{ref}}(t) &= 0.15\pi \left(1 - \cos \left(\frac{2\pi t}{5} \right) \right) & \text{and } \omega_{\text{ref}}(t) &= -v_{\text{ref}}(t)/1.5 \\
30 \text{ s} \leq t < 35 \text{ s} : v_{\text{ref}}(t) &= 0.15\pi \left(1 - \cos \left(\frac{2\pi t}{5} \right) \right) & \text{and } \omega_{\text{ref}}(t) &= v_{\text{ref}}(t)/1.5 \\
35 \text{ s} \leq t < 40 \text{ s} : v_{\text{ref}}(t) &= 0.15\pi \left(1 - \cos \left(\frac{2\pi t}{5} \right) \right) & \text{and } \omega_{\text{ref}}(t) &= -v_{\text{ref}}(t)/1.5 \\
40 \text{ s} \leq t < 45 \text{ s} : v_{\text{ref}}(t) &= 0.15\pi \left(1 - \cos \left(\frac{2\pi t}{5} \right) \right) & \text{and } \omega_{\text{ref}}(t) &= v_{\text{ref}}(t)/1.5 \\
45 \text{ s} \leq t < 50 \text{ s} : v_{\text{ref}}(t) &= 0.25 \left(1 + \cos \left(\frac{\pi t}{5} \right) \right) & \text{and } \omega_{\text{ref}}(t) &= 0 \\
50 \text{ s} \leq t : v_{\text{ref}}(t) &= 0.5 & \text{and } \omega_{\text{ref}}(t) &= 0
\end{aligned}$$